ELSEVIER

PII: S1359-835X(97)00004-3

Composites Part A **28A** (1997) 529–547

1359-835X/97/$17.00

Stress analysis and strength prediction of mechanically fastened joints in FRP: a review

P. P. Camanho and F. L. Matthews*
Centre for Composite Materials, Imperial College of Science, Technology and Medicine, London SW7 2BY, UK
(Received 22 July 1996; revised 16 December 1996)

A review of the investigations that have been made on the stress and strength analysis of mechanically fastened joints in fibre-reinforced plastics (FRP) is presented. The experimental observations of the effects of joint geometry, ply-orientation, lay-up and through-thickness pressure on the joint behaviour are described briefly for both single and multi-fastener joints. The analytical and numerical methods of stress analysis required before trying to predict failure are discussed. The numerical approaches cover both two and three-dimensional models and the effects of clearance, friction and geometry are assessed. The several methods that have been used to predict failure in single or multi-fastener joints are described. It is concluded that there are some issues that require further investigation. There is no general agreement about the method that should be used to predict failure, but progressive damage models are quite promising since important aspects of the joint's behaviour can be modelled using this approach. In order to take into consideration several factors related to joint strength the use of three-dimensional models is suggested. These models require a three-dimensional failure criterion and an appropriate property degradation law. © 1997 Elsevier Science Limited

(Keywords: mechanically fastened joints; composite laminates)

INTRODUCTION

A large part of the research that has been done on mechanically fastened joints has been concerned with the experimental determination of the influence of geometric factors on the joint strength. The usual procedure is testing specimens until final failure, varying the factor under study and keeping the other factors constant.

There are five common failure modes in mechanically fastened joints in composite laminates, namely tension, shear, bearing, cleavage and pull-through, as shown in *Figure 1*. Associated with these failure modes, the planes shown in *Figure 2* are defined. This figure also shows the circumferential co-ordinate direction, θ.

Hart-Smith[1] considered that net-tension failure occurs when the bolt diameter is a large fraction of the strip width. This fraction depends on the type of material and lay-up used. Bearing failure occurs predominantly when the bolt diameter is a small fraction of the plate width. This mode of failure leads to an elongation of the hole. Shear-out failure can be regarded as a special case of bearing failure. This mode of failure can occur at very large end distances for highly orthotropic laminates. Cleavage failures are associated with both an inadequate end distance and too few transverse plies. Pull-through failure occurs mainly with countersunk fasteners or when the thickness to diameter ratio is sufficiently high to precipitate failure.

Several authors[1–6] have highlighted the importance of width (w), end distance (e), hole diameter (d) and laminate thickness (t) on the joint strength.

Kretsis and Matthews[2] showed, using E glass fibre-reinforced plastic (GFRP) and XAS carbon fibre-reinforced plastic (CFRP), that as the width of the specimen decreases, there is a point where the mode of failure changes from one of bearing to one of tension. This change leads to a considerable drop in the load capacity of the joint.

A similar behaviour between the end distance and the shear-out mode of failure was found. As the end distance decreased the bearing failure mode changed to one of shear-out, with the corresponding decrease in joint strength.

Collings[3] tested CFRP for a range of laminate configurations and hole sizes, and investigated the relation between joint strength and w/d, e/d and t/d. The general trends obtained were in agreement with Kretsis and Matthews[2] work. The minimum values of w/d and e/d needed to achieve full strength were dependent upon the lay-up used. The effect of laminate thickness on bearing strength was shown to be insignificant provided that a minimum value of through-thickness compression of 22 MN/m^2 was applied over the washer contact area. This result for CFRP is in contrast with the result obtained[2] for GFRP.

* To whom correspondence should be addressed.

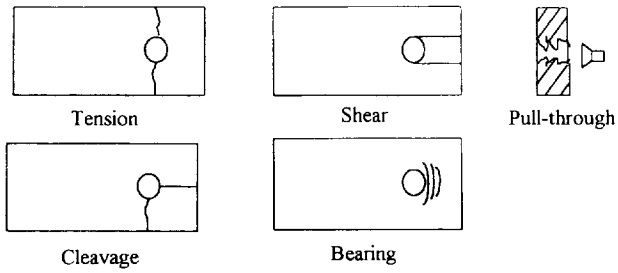

Figure 1 Failure modes

Hart-Smith[1,4] used a different approach to study the behaviour of bolted joints. A simple theory to calculate the elastic stress concentration factors at loaded holes was used. Combining this analysis with tests on composite materials to account for the stress concentration relief that occurs in laminates prior to failure, a considerable generalisation to geometries for which data was not available was achieved. The results obtained showed an increase in the joint structural efficiency for decreasing *d/w* values, until an optimum value was achieved. As in Kretsis and Matthews[2] work, the failure mode changed from tension to bearing. It was assumed that delamination eventually occurs near the hole. The presence of such damage reduces the stress concentration factor near the hole. As larger holes undergo proportionally less stress concentration relief prior to failure this effect is related to the reduced strength of larger holes. For this reason the author suggested the use in graphite-epoxy laminates of glass fibre softening strips located near the hole, of four bolt diameters width, in order to increase the stress concentration relief due to the greater delaminations associated with glass fibres.

Hodgkinson *et al.*[5] presented failure data for several types of joints in Kevlar fibre-reinforced plastics (KFRP). As in CFRP and GFRP, small values of end distance resulted in shear-out failures and small values of width resulted in tensile failures.

Collings[3] demonstrated that the tensile strength of a single-hole joint is strongly dependent on ply orientation. Testing CFRP laminates balanced about the mid-plane, the author concluded that in (0°/ ± α°) laminates the bearing strength was dependent on the ratio of 0° plies to ± α° plies, and the effect of these plies was dependent on the type of failure. The fibre orientation angle, α, is defined in *Figure 3*.

In other work, Collings[6] showed that in CFRP the addition of ± 45° plies to a 0° or 90° laminate increased the bearing strength until the ± 45° plies account for approximately 75% of the total laminate thickness. The author considered that the presence of ± 45° plies reduces

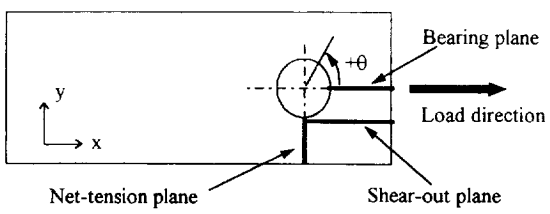

Figure 2 Definition of failure planes

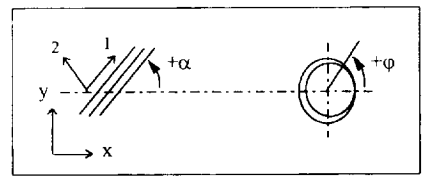

Figure 3 Definition of fibre orientation and contact angle

the stress concentration factor. The addition of either 0° or ± 45° to a 90° laminate produces a similar change in the variation of the bearing strength.

Kretsis and Matthews[2] demonstrated the same effect in GFRP. They concluded that the lay-up had a great effect on both joint strength and failure mechanism. The minimum values of *w/d* and *e/d* to achieve full strength depend on the lay-up used. High *w/d* and *e/d* values were necessary to achieve full strength in (± 45°) and (0°/90°) laminates respectively.

Hart-Smith[1,4] concluded that shear-out failures are prevalent for fibre patterns which are both rich in 0° and deficient in 90° plies. The same strength and failure modes were achieved in joints with 50% of 0° plies and 50% of ± 45° plies for $e/d = 2$ and $e/d = 22$. The author concluded that shear-out and bearing strengths are maximised for quasi-isotropic laminates. As a general rule, he stated that there should never be more than 3/8 nor less than 1/8 of the fibres in any one of the basic laminate directions: ± 45°, 0° and 90°.

Collings[3] showed that the bearing strength of CFRP could be improved by increasing the lateral (i.e. through-thickness) compressive stress around the loaded hole. This stress (or "constraint pressure') which is assumed constant over the washer area, was obtained using the following expression:

$$\sigma_{zz} = \frac{T}{0.2d\frac{\pi}{4}(D^2 - d^2)} \quad (1)$$

D and d are, respectively, the washer and hole diameter and T is the applied torque. For (0°/ ± 45°) laminates improvements from 60% to 170% according to hole size were achieved with constraint pressures of up to 22 MN/m^2. At higher constraint pressures little further improvement was achieved. It was considered that lack of through-thickness compression at the contact zone could lead to premature in-plane compressive failure. Failure occurred by initiation of shear cracks at the hole edge and subsequent propagation to the edge of the clamped region.

The same effect was found by Kretsis and Matthews[2] in GFRP. If the laminate is restrained laterally, the zone under the washers develops shear cracks but is not allowed to expand under compression. Therefore the lateral expansion is spread into a wider area that lies outside the washer boundary. For high values of clamping pressure the bearing strength-clamping pressure relation was almost constant, suggesting the existence of an optimum value of pressure that should be applied. To avoid unnecessary damage in the laminate this value should not be exceeded.

Godwin *et al.*[7] considered that the joint strength depends

on the through-thickness restrain offered by the fastener. A plain pin will give the lowest bearing strength and a fully tightened bolt the highest bearing strength. The bearing strength obtained using a riveted joint would fall between these extremes.

Hart-Smith[1,4] related the effect of bolt tightening to the higher bearing strength of the laminate in the middle of a double-shear lap, compared with the laminates in the outer laps. This was a result of the better confinement of the damage in the inner lap. This effect leads to the conclusion that joint strength depends not only on the amount of bolt clamping, but also on the area over which is applied. The influence of clamp-up is not as pronounced for the other failure modes as it is for the bearing failure.

Quinn and Matthews[8] measured the pin-bearing strength of GFRP using specimens with mid-plane symmetry. Eight different stacking sequences of laminates with 0°, 90° and ± 45° layers were analysed. The joint strength was found to be dependent upon the stacking sequence. This effect is due to the through-thickness direct and shear stresses that occur at the hole boundary. The magnitudes of these stresses are dependent on the stacking sequence. The results suggested that placing the 90° layer at the surface increases the bearing strength. Placing a 90° layer at the surface of the specimen will produce a compressive through-thickness direct stress that can inhibit delamination. Clearly, the interlaminar shear stress also influences the failure characteristics.

This effect was also shown in CFRP by Collings[2] who concluded that less homogeneous stacking sequences exhibited lower bearing strengths, due to the high interlaminar shear stresses that occur in such laminates.

In the majority of practical applications, the load transferred between two components is in multi-row fastener patterns. The preceding discussion has dealt with either single-bolt joints or with individual bolts isolated out of a single row, by representing the latter as a single bolt in a strip of a width equal to the bolt pitch. Collings[3] stated that this approach is valid for sufficiently large pitches where there is no interference of stress fields around the holes. In this case it was possible to predict the total load carried by multi-hole joints using single-hole data.

Hart-Smith[1,4] concluded that a multi-hole joint did not offer a substantial improvement over a single-hole joint. In order to increase the joint strength above the optimum tension failure for a single bolt it would be necessary to bring about a great reduction in bearing stress and an increase in the ratio of pitch to diameter (p/d). Whereas two bolts could improve the strength of an optimally proportioned single-bolt joint by about 10%, a line of eight or ten bolts would be necessary to achieve a 25% improvement. The strongest joint which could fail in bearing had only one row of bolts in it. Multi-row joints can decrease the bearing stress but can also lead to a tension failure.

An appreciation of the experimental behaviour is necessary before attempting a stress analysis or failure prediction. Thus, knowledge of the modes of failure and the influence of geometric and other parameters, as described above, form an essential precursor to any theoretical study.

The approaches to be reviewed below cover both classical (continuum) and numerical (mainly finite element) methods.

ANALYTICAL METHODS OF STRESS ANALYSIS

The analytical deduction of the stress distribution around a frictionless pin-loaded hole based on the complex function method developed by Muskhelishvili[9], and adapted to orthotropic materials by Lekhnitksii[10], was performed by de Jong[11]. The pin was assumed rigid, the uniformly distributed load in the plate was applied at an infinite distance, and a cosinusoidal radial stress distribution represented the pin-hole interaction. As shown in *Figure 4*, the solution was obtained as the combination of two load cases. Firstly, a pin-loaded hole, where loads with the same direction and value were applied at the plate edges. The series coefficients were calculated using the boundary conditions in the assumed loaded zone of the hole. The other case was an open hole where the loads with the same value but with opposite directions were applied at the plate edges. Results were obtained for unidirectional, quasi-isotropic and ($0°_4$ / ± 45°) CFRP laminates, using w/d ratios of 2.5, 5 and ∞. It was shown that the direct stress distribution at the hole boundary was highly dependent on the lay-up and width used. The maximum value of the direct stress occurred in the unidirectional laminate, for $w/d = 2.5$, in the vicinity of the net-tension plane. Qualitatively, this result is in agreement with experimental results[1–4]. The decrease of the direct stress in the net-tension plane was more pronounced for the highly orthotropic laminate, whilst in the bearing plane the opposite effect occurred. The results have to be corrected to account for effects of finite end distance.

In order to account for the effect of friction at the pin-hole boundary, Zhang and Ueng[12] developed a method in which direct and shear stresses at the hole boundary were obtained using Lekhnitksii's[10] method from displacement expressions which satisfied prescribed conditions. Infinite dimensions were considered and the solution resulted from the superposition of two load cases. The stress distributions at the hole boundary for several friction coefficients for a ($0°_4$ ± 45°)$_s$ laminate are shown in *Figure 5*. Such distributions were also obtained for (± 45°)$_s$, ($0°_3$ / ± 45°)$_s$, ($0°_4$ / ± 45°)$_s$ and ($90°_4$ / ± 45°)$_s$ laminates. It was concluded that these stress distributions were dependent on the lay-up and on the presence of friction. As friction increased, the shear stress, $\sigma_{r\theta}$, along the hole edge increased steadily and the direct

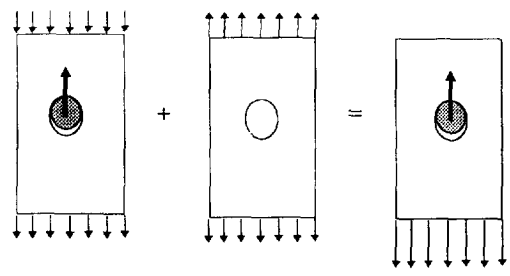

Figure 4 Superposition of load cases[11]

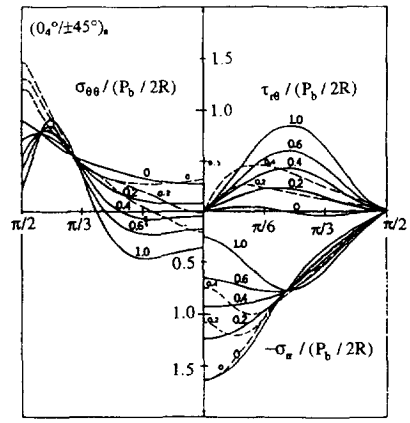

Figure 5 Stress distributions around a pin-loaded hole in a $(0°_4/\pm 45°)_s$ laminate[12]

stress, σ_{rr}, decreased in an area near $\theta = 0°$. The size of this area depends on the ratio of the moduli of elasticity along the two principal axes. Near $\theta = 0°$, the hoop stress, $\sigma_{\theta\theta}$, may vary gradually from tension to compression or increase in compressive value as friction is increased. The maximum value of $\sigma_{\theta\theta}$ also increased with increasing friction.

A detailed investigation into the effects of friction, pin elasticity and clearance on the stresses near the pin-loaded hole was made by Hyer and Klang[13,14]. An infinite plate was loaded by a pin, by shear stresses which were assumed to be spatially uniform over its cross-sectional area. As in previous investigations, the elasticity problem was formulated in terms of complex variable theory. Boundary and inferface conditions were prescribed for the no-contact region, no-slip region and slip region. The unknown coefficients of the complex series that represented boundary tractions were determined using a collocation and iteration procedure. CFRP laminates with the (0°), (90°), $(0°/\pm 45°/90°)_s$, and $(0°_2/\pm 45°)_s$ configurations were analysed. It was concluded that the pin flexibility was not an important factor in determining the stress distribution in a pin-loaded hole. As for de Jong's[11] results, the degree of orthotropy strongly influenced the peak stresses and the stress distributions. A comparison of results was made with those obtained using the often assumed cosinusoidal stress distribution in the hold boundary. It was concluded that the cosinusoidal stress distribution was not generally accurate. The effects of friction were in agreement with those previously described[12]. The most significant effects of increasing clearance was moving the peak circumferential stress toward $\theta = 0°$ and increasing the peak radial stress.

A method for the calculation of stresses in anisotropic plates with a row of equally spaced pin-loaded holes was presented by de Jong[15]. The solution of the problem was based on two load systems, namely a plate with a row of open unloaded holes and a plate with a row of pin-loaded holes. Unlike in de Jong's previous work[11], the pin-hole interfacial stresses are calculated rather than assumed and the effect of friction is considered. As expected, when decreasing the pitch to diameter ratio (*p/d*) the tangential stress concentration factor in the net-section increased, but was almost constant at $\theta = 0°$. The radial stresses decreased at the latter location. The effect of friction was in general agreement with the results obtained by Hyer and Klang[13]. It should be noted that, due to limited areas of convergence, these solutions were confined to the edge of a hole and its direct vicinity. Physically, a joint with a few pins or the end pin of a joint cannot be represented because of the assumptions in the theory.

NUMERICAL METHODS OF STRESS ANALYSIS

Stress distribution in pin-loaded holes: two-dimensional models

Several authors[16–23] considered a plane stress state in a pin-loaded plate. Usually, two-dimensional finite element models were created and classical lamination theory[24] was applied. Clearly, the effects of clamping pressure and stacking sequence cannot be studied with this approach. Several methods can be used to deal with the pin-hole contact problem. Some authors assumed a value for the contact angle[16] ϕ (defined in *Figure 3*). This procedure has the advantage of simplicity but is not accurate for a clearance fit since the contact angle varies non-linearly with load. The contact zone can be calculated using elements connecting the nodes on the hole boundary to a node at the hole centre, using beam or rigid link elements[25]. The nodes connecting the beam or rigid elements which were in tension were assumed to be in the non-contact zone (radial separation between pin and hole boundary). The usual procedure is to use iterative[16–20] or inverse methods[21–33]. Iterative methods allow the determination of the relation between the area of contact with load, with the possibility of considering friction. Using this technique, for each load magnitude the contact region is unknown. For each load increment the boundary nodes are checked for contact with the pin and, when friction is present, the position of the contact nodes either in the slip or no-slip region are determined. Although the contact problem is non-linear, inverse methods require only linear finite element analysis, resulting in simpler models than the ones created using iterative methods. Displacement constraint equations are specified along the bolt-hole interface and stress boundary conditions are specified at the end of the contact arc and in the region beyond the contact arc. A value for the contact angle is assumed and using the previously defined conditions the corresponding load is calculated. The process is repeated for a series of prescribed contact angles, and the pairs of contact angle and corresponding load are plotted. It should be noted that this method is only applicable when geometric and loading symmetries exist.

The effect of clearance on the stress distribution near the loaded hole was investigated by Naik and Crews[21]. Using an inverse formulation, assuming a frictionless contact and a rigid pin loading a quasi-isotropic laminate, it was shown that the contact angle was a function of clearance. This relation is shown in *Figure 6* where c_d is the diametral clearance between the hole and the bolt. For constant bearing stress, increasing the clearance decreased the

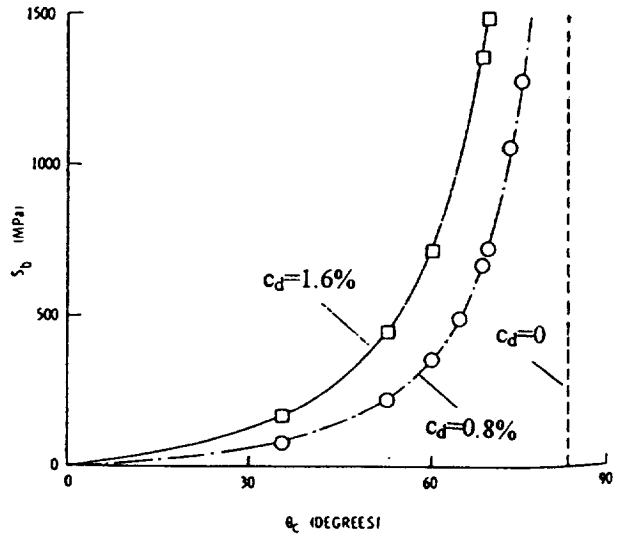

Figure 6 Effect of clearance on the relationship between bearing load and contact angle[21]

contact angle. As shown in *Figure 7*, for a bearing stress of 475 MPa, the clearance also influenced the value and position of the maximum radial and hoop stresses. The maximum values of these stresses increased with increasing clearance. When clearance is present, the relations of the radial and hoop stresses with bearing stress are initially (small loads) non-linear, becoming linear with increasing bearing stresses. For a perfect-fit joint, these relations are linear and the contact angle is constant.

Ramamurthy[22,23] used an inverse technique to study the behaviour of pins fitted with interference. This kind of joint is sometimes used to increase the fatigue life of metallic structures. Assuming a frictionless contact and a rigid pin, it was concluded that the maximum bearing stress varies nonlinearly with the load. For high loads, radial stresses are higher and hoop stresses are lower when compressive loads are applied at the laminate border. No comparisons between stress distributions for the cases of clearance, perfect-fit and interference were made.

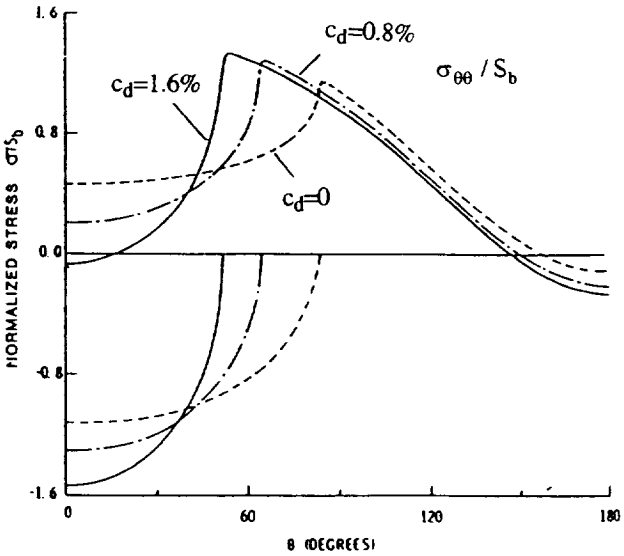

Figure 7 Effect of clearance on hole-boundary stresses[21]

A comprehensive study of geometrical effects on the stress distribution of a pin-loaded plate was done by Crews *et al.*[19]. A frictionless contact and perfect-fit pin were assumed and six laminates were considered: (0°/ ± 45°/90°), (0°), (90°), $(0°/90°)_s$, $(\pm 45°)_s$, and $(0°/\pm 45°)_s$. The stress distributions around the hole boundary were represented, showing the strong influence of anisotropy on both magnitude and location of the peak hoop stress on the hole boundary. It was considered that the hoop stress, $\sigma_{\theta\theta}$, the radial stress, σ_{rr}, and the shear stress, σ_{xy}, were associated with the net-tension, bearing and shear-out failures respectively. The effect of *w/d* was predominant on the hoop stress. As a result, the main influence of *w/d* will be in the net-tension failure mode. A tensile stress concentration factor, K_{tb}, was defined as the ratio of the maximum hoop stress, $(\sigma_{\theta\theta})_{max}$, that occurred near the end of the contact arc, to the bearing stress, S_b:

$$K_{tb} = \frac{(\sigma_{\theta\theta})_{max}}{S_b} \tag{2}$$

In *Figure 8* it is shown that for a constant value of end distance K_{tb} increases with decreasing *w/d*. Decreasing *e/d* increased both the hoop and shear stresses. The effect on the shear stress may be important in laminates with small shear strengths, like the (0°) laminate. The shear stress concentration factor is defined by:

$$K_{sb} = \frac{(\sigma_{xy})_{max}}{S_b} \tag{3}$$

As shown in *Figures 9 and 10*, both K_{sb} and K_{tb} increase with decreasing *e/d*. The edge distance only weakly influenced the peak values of bearing stress. These conclusions are qualitatively in good agreement with experimental results[1-4].

The effects of friction, geometry, clearance and material properties on load distribution were investigated by Rowlands *et al.*[18]. Using an iterative procedure previously defined[17] and assuming a rigid pin, the finite element model was substantiated by comparing the results with Moire and strain gauge experimental results. It was concluded that a

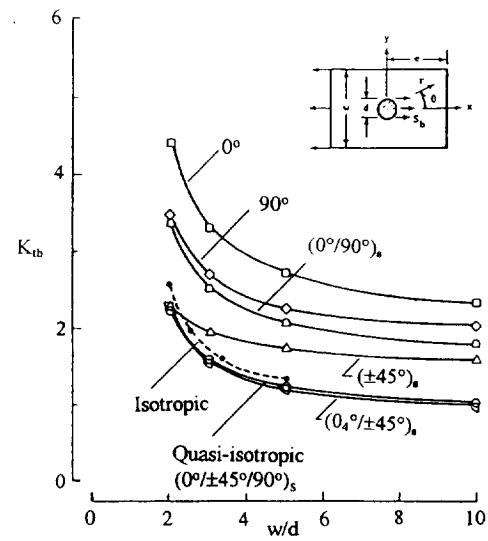

Figure 8 K_{tb} as a function of *w/d*, for *e/d* = 10[19]

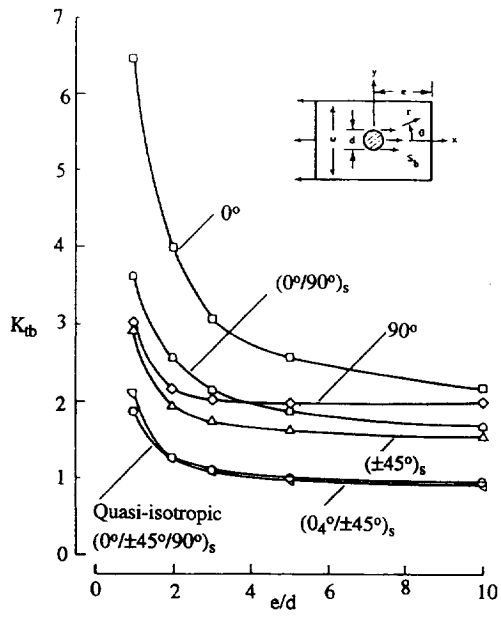

Figure 9 K_{tb} as a function of e/d, for $w/d = 20$[19]

change in contact friction from $\mu = 0.7$ to $\mu = 0.4$ had little effect on the radial stress at the hole boundary. This result is in disagreement with the results obtained by Zhang and Ueng[12] and Hyer and Klang[13]. As the stiffness of the material increased (from glass fibres to boron fibres), the peak radial stress increased. This effect explains partially the use of softening materials near pin loaded holes, as described by Hart-Smith[1] and Kretsis *et al.*[2]. As in Naik and Crews[21] work, it was shown that increasing clearance increased contact radial stresses. For $e/d \leq 4$ the stress distribution was only slightly affected by variations in end distance. This result is in qualitatively agreement with experimental results[3].

Using an iterative method, Eriksson[20] investigated the effects of clearance, friction and bolt stiffness on the stress distribution near the hole boundary and arrived at the same conclusions as Hyer and Klang[13]. In Eriksson's work, the stress distributions were also obtained along an arc at a distance $a_0 = 1.26$ mm from the hole boundary. This distance is associated with a strength criterion that will be described later. As at the hole boundary, the stress distribution along this arc was strongly dependent on the laminate properties. The same effect occurred for shear stress on the shear-out plane and for bearing stress on the bearing plane. The effect of friction, along the arc considered, followed the same trends as at the hole boundary for the hoop stress, but had a different effect in the shear stress. At a_0, the presence of friction decreased the shear stresses.

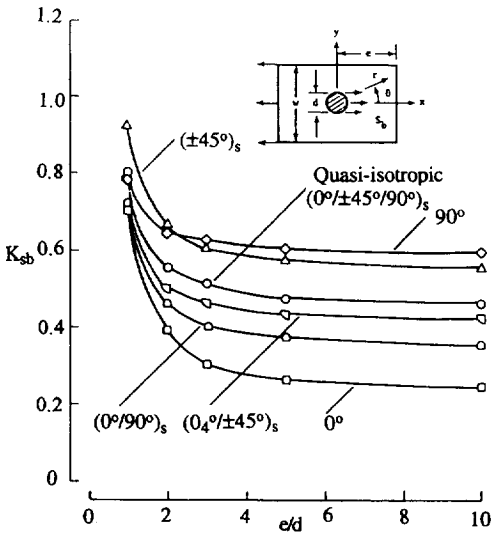

Figure 10 K_{sb} as a function of e/d for $y = d/2$ and $w/d = 20$[19]

Stress distribution in pin-loaded hole: three-dimensional models

As shown by experimental analysis, through-thickness effects play a substantial role on joint strength. In order to model these effects, more complicated three-dimensional finite element models are required.

Matthews *et al.*[25] investigated the effect of the way the load is transmitted to the plate on the stress distribution around a loaded hole in a (0°/ ± 45°/0°)$_s$ laminate. Using a three-dimensional finite element model and assuming a perfect-fit rigid pin and frictionless contact, three configurations were considered: pin-loaded hole, finger-tight bolt and fully tightened bolt. Significant differences in stress distributions were obtained. In the pin-loaded case, the maximum through-thickness tensile stress, σ_{zz}, was found to be about 7% of the bearing stress. It was concluded that this effect can be related to the experimental results, since failure occurs in the region of maximum σ_{zz} due to splitting between layers. The distribution of σ_{xx} around the hole showed good agreement with results obtained by de Jong[11]. For the finger-tight bolt, a general reduction of σ_{zz} within the washer area was noticed. In a fully tightened bolted joint, significant through-thickness compressive stress was present. The interlaminar shear stress, σ_{zx}, was found to increase at the washer edge. This effect was related to the experimental results where failure occurs by delamination at the washer edge. These results are also consistent with experimentally observed relative strengths.

The effects of friction, clamping pressure, clearance and stacking sequence were investigated by Chen *et al.*[26]. An incremental variational principle was formulated and a general finite element technique satisfying contact conditions was established for the three-dimensional contact stress analysis. Three cases were considered. Firstly, a thin CRFP (45°/0°/ − 45°/90°)$_s$ laminate subjected to a bolt load and clamping pressure was analysed to evaluate the accuracy of the model. Comparing with experimental results obtained by Smith *et al.*[27] reasonable results were achieved. The previously described effects are studied in a thick (0°/90°)$_s$ or (90°/0°)$_s$ GFRP subjected to a bolt load. The effects of friction, clearance and bolt elasticity are in agreement with the results obtained by Hyer and Klang[13,14]. A much lower tensile interlaminar normal stress on the bearing plane, σ_{zz}, was observed in the (90°/0°)$_s$ laminate and this can prevent delamination. This result helps to explain the higher bearing strength of laminates with 90°

layers at the laminate surface, as experimentally demonstrated by Quinn and Matthews[8]. As in the work of Matthews *et al.*[25], the main effect of the clamp-up applied by washers was to induce lower interlaminar tensile direct stress or higher interlaminar compressive direct stress near the hole. The effect of clamp-up is not investigated at the outer edge of the washer. The third case was the analysis of the delamination onset for GFR $(0°_6/90°_6)_s$ or $(90°_6/0°_6)_s$ laminates and will be discussed later.

Marshall *et al.*[30] investigated the effects of friction, clamping and laminate stiffness on the stress distribution in $(0°/90°)_s$ and $(90°/0°)_s$ GFRP and CFRP laminates. Results were obtained for pin-loaded holes and for bolted joints with several degrees of clamping. The effect of friction was investigated in the pin-loaded hole. The finite element model was validated comparing numerically determined strains with strains obtained using strain gauges, on the bearing plane. The results were in reasonable agreement. Only the frictionless and infinite friction cases were considered, showing the reduction of axial interface stresses in the bearing plane when friction is present. This result is consistent with previous analysis[13,20]. It was concluded that increased friction redistributes the load and correspondingly the position of the main load-carrying fibres away from the bearing plane towards the net-tension plane. The stress distributions of GFRP showed similar profiles as compared with CFRP, but with marked drops in all stresses. These reductions are related to the lower stiffness of GFRP fibres. The effect of stacking sequence was in agreement with the results obtained by Matthews *et al.*[25]. A general improvement in all the stress profiles was obtained using bolted joints. The effect of clamping pressure was in good agreement with the results obtained by Matthews *et al.*[25].

The effect of intralaminar non-linear shear behaviour on the modelling accuracy of pin-loaded $((0°/90°)_n)_s$ and $((+45/-45)_n)_s$ GFRP laminates was investigated by Sarabian[28]. A three-dimensional finite element model was created using ABAQUS software. The pin-plate interaction was modelled using gap contact elements and a frictionless contact was assumed. Although being a factor with small influence on the stress distribution near a pin-loaded hole[13,14], pin elasticity was considered. The non-linear shear behaviour was determined from the ASTM D3518-76 specification. This test allowed, using a least squares curve fit procedure, the derivation of a relation between the shear stress and the shear strain that was implemented in the finite element model constitutive equation. In order to assess the effect of this non-linear behaviour, a three-dimensional finite element linear model was also created. It was found that both radial and hoop stresses at the hole boundary were significantly affected by the inclusion of material non-linearity. A reduction of the maximum shear stress was observed in the shear-out section of the $((0°/90°)_3\,0°)_s$ laminate and in the net section of the $((+45/-45)_3)_s$ laminate. Through-thickness direct stresses were found to be negligible in comparison with in-plane stresses, and increased when material non-linearity was assumed. Using the Moire technique experimentally determined strains were found in the shear-out plane of the $((0°/90°)_3/0°)_s$ laminate and in the net and bearing planes of the $((+45/-45)_3)_s$ laminate. The results obtained validated the importance of including non-linear material behaviour in these laminates. However, one must be cautious when using the non-linear shear stress–strain data from the ASTM D3518-76 type specimen. Much less non-linearity is observed in other specimens, such as the ASTM D4255 type specimen or 10° off-axis specimen.

The influence of the lay-up on the stress distribution in a pin-loaded plate was investigated by Barboni *et al.*[29]. Assuming the displacements as a function of a power series expansion of the z co-ordinate in the thickness direction allows the three-dimensional character of the analysis to be handled without adopting classical three-dimensional numerical procedures. This procedure reduces computation time. A cosinusoidal load distribution was assumed at the pin-hole boundary. The different distributions of σ_{zz} around the hole boundary are shown for $((0°/90°)_6)_s$ and $(0°/\pm 45°/90°)_s$ laminates. It should be noticed that the cosinusoidal stress distribution was found by several authors to be satisfactorily accurate only in quasi-isotropic laminates. Considering also the influence of the non-linear intralaminar shear behaviour that occurs in cross-ply and angle-ply laminates[28], we should consider the results obtained for the $((0°/90°)_6)_s$ laminate as only a poor approximation.

Three-dimensional finite element models have the drawback of being computationally expensive and, when modelling a laminate using one three-dimensional element per layer (stacked bricks models), problems related to the aspect ratio of the elements can arise. One way to overcome these problems is to use a new three-dimensional method based on spline approximations that has been proposed by Iarve[31]. The minimum potential energy principle and the Lagrange multiplier method were used. The contact condition was formulated as radial displacement continuity between the plate and the bolt and the Lagrange multiplier was interpreted as the value of the contact stress. Based on the work previously done[32] on plates with open holes, new spline approximations of the plate x,y,z displacement components were obtained. Spline approximations for the bolt displacement and for the Lagrange multiplier were also obtained. By differentiation of the displacement approximations and using Hooke's law, the total potential energy can be expressed as a function of spline approximation coefficients. A $(0°/+45°/-45°/90°)_s$ laminate loaded by a rigid pin was investigated. Frictionless contact was assumed and the distributions of normalised radial stress and polar displacement were obtained for zero clearance and 4% clearance. As concluded by other authors[21], a clearance fit leads to an increase of normalised radial stresses and a reduction of the contact angle.

Multi-fastener joints

The numerical investigations of stress distributions in multi-pin joints found in the literature were based on two-dimensional finite element models. Both lines (parallel to the load) or rows (perpendicular to the load) of fasteners have been considered.

Wang and Han[33] investigated the load proportioning in multi-row joint fasteners using a two-dimensional finite element model. A single-lap joint of two symmetric laminates with several fastener configurations was considered. The fasteners were modelled using a proposed pure shear element. Assuming linear elastic behaviour, the joint behaviour was considered as the sum of two loading cases and a factor f_i was defined as the ratio of load carried by a fastener to the average load. This factor represents the unevenness of load distribution between fasteners. Not surprisingly, the results showed that in the case of a line of fasteners, the first and last fastener are the ones subjected to the highest loads. It was concluded that as the axial stiffness of the plates decreases or as the total number of fasteners in the axial or transverse direction increases the load distribution tends to be more uneven.

A more comprehensive work about load proportioning was made by Griffen *et al.*[34]. Considering double lap joints, ABAQUS software was used to create two independent two-dimensional finite element models, one representing the composite inner lap and one representing the steel outer laps. The laps interact by means of circular rigid surfaces and gap elements. Two-row joints with three-hole, five-hole, seven-hole and nine-hole geometries with shifted centres were analysed. It was found that load proportions were not substantially affected by the level of applied load. As the number of fasteners increases, the load proportioning becomes more equal. This result contrasts with the results of Wang and Han[33]. The outboard row carried a substantially larger portion of the load in the narrow specimen, with a shift to the inboard row carrying a slightly larger portion in the wider specimen. The different distributions of radial contact stresses on outboard and inboard row holes were shown. Specially instrumented pins and strain gauges were used to verify the numerical results, and good agreement was achieved.

In multi-row joints, fastener holes are subject to bearing loads and by-pass loads that are reacted elsewhere in the joint. The effect of this type of loading on the stress distribution of a frictionless hole loaded by a rigid pin was investigated by Naik and Crews[35]. Using the previously developed inverse technique[21] and considering the effect of bolt-hole clearance and a sufficiently large pitch to avoid interactions between holes, tensile and compressive loads were analysed for a single hole. A coefficient β was defined as the ratio of bearing stress, S_b, to the by-pass stress, S_{np}:

$$\beta = \frac{S_b}{S_{np}} \tag{4}$$

These stresses are defined by

$$S_b = \frac{P_b}{dt} \tag{5}$$

$$S_{np} = \frac{P_{bp}}{(w-d)t} \tag{6}$$

where P_b and P_{bp} are, respectively, the load at the hole and the by-pass load. This coefficient was found to have a significant effect on the contact angle and peak stresses around the hole. For a given bearing stress it was found that increasing the tensile by-pass load (reducing β) resulted in an increased contact angle φ, whilst increasing the compressive by-pass loading had the opposite effect. When a tensile by-pass load was applied, the peak value of radial stress was not very sensitive to S_{np}, whereas its distribution showed the variation of the contact angle. With increasing S_{np} the hoop stress rises significantly, its maximum being located a few degrees beyond the contact region. In the case of compressive loading, the radial stress rises nearly proportionally with S_{np}. As the absolute value of S_{np} increases the peak value of the hoop stress becomes compressive. It was concluded that compressive loading can lead to dual contact between the hole and the bolt. This contact occurred for values of β between 0 and -3. An important consequence of this kind of contact is that it allows load transfer across the bolt and therefore reduces the stress concentration around the hole. It should be noticed that these results were obtained for constant values of S_b. This means that when S_{np} increases the total load applied to the joint also increases. More relevant results would be obtained if the total load applied was considered constant and the influence of the ratio between bearing and by-pass loads investigated.

Using an unusual approach, Kim and Kim[36] investigated two bolts in a line and in a row. Using extended interior penalty methods, the variational formulation obtained was discretized using the finite element method. A frictionless contact was assumed between a rigid pin and the laminate with symmetric stacking sequence. Three laminates were considered: (0°), (90°) and $(0°/\pm 45°/90°)_s$. The situations of clearance and perfect fit were analysed for the $(0°/\pm 45°/90°)_s$ laminate, whilst clearance was present in the other laminates. For the two holes in a line it was concluded that the width and length of the plate and the pitch distance have a significant influence on the distribution of contact pressure. The hole nearest to the applied force experiences more load and a wider contact area than the other hole. In a perfect fit situation the hole at the greater distance from the load has the widest contact area. The results obtained for two holes in a row showed similar characteristics compared with those of single holes. The contact area moves towards the symmetric axis of the plate and, as shown in *Figure 11*, when the hole moves to the left the location of maximum contact pressure moves to the right, and vice versa.

STRENGTH PREDICTION METHODS

Several approaches have been used to predict the strength of composite laminates with fastener holes. Most of the methods developed are based on two-dimensional models and only recently have methods considering three-dimensional models been developed. The determination of the joint strength depends on the definition of failure. This definition can vary from the maximum load sustained by the joint to a criterion based on the deformation of the hole. According to Godwin and Matthews[37] the majority of

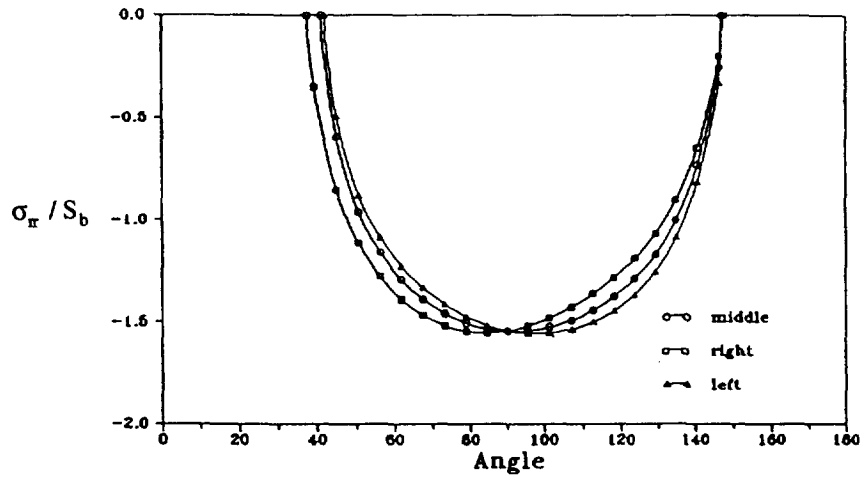

Figure 11 Variation of contact stress distributions for different distances from the symmetric axis of the plate[36]

authors seem to agree on the advisability of a definition based on the latter criterion, but the values that should be used vary significantly. Other definitions like the first peak or the first non-linearity in the load–displacement plot, and the load at which cracking is initiated were suggested by Johnson and Matthews[38].

Failure theories

Methods based on both hole boundary stress distribution and failure theories[39–42] were among the first methods used. In these methods, the peak local stresses are used in a failure theory to predict laminate strength.

Waszczak and Cruse[39] adopted the maximum stress, maximum strain and distortional energy criterion. A frictionless contact and a cosinusoidal boundary radial stress distribution were assumed. When the failure criterion was satisfied for one lamina, that lamina was assumed to have failed and was removed from the analysis. The stress distribution and failure criteria are then recalculated and the procedure repeated until total laminate failure occurred. Using this procedure conservative results were obtained and the failure modes were not predicted.

The typical conservative predictions obtained using failure theories are related to the localised damage that occurs near the hole prior to the laminate failure. This effect was experimentally reported by Hart-Smith[1]. This author showed that the effective stress concentrations at laminate failure are smaller than the elastic stress concentration and considered that the prime factor that leads to this stress concentration relief is delamination. This effect is also related to the well known hole-size effect that occurs in laminates with unloaded holes. This effect is characterized by a strength decrease for larger hole sizes in laminates without finite dimension effects. Explanations for this effect were given by Crews[43], who considered that the localised damage that occurs prior to failure reduces the laminate stiffness in that zone, and consequently reduces the stress concentration, is more effective for small holes. At these holes, the regions of high stress concentrations are small and readily influenced by the damage at the hole boundary. A second explanation given by the author was that for large holes a higher volume of material is highly stressed and the probability of containing a large flaw that can lead to failure is higher than for small holes. A similar explanation was given by Whitney and Nuismer[44] who related the hole size effect to the stress distributions around holes of different sizes in infinite plates. Although the computed stress concentration factors at the edge of the hole were the same for all hole sizes, the stress distribution was much steeper in the case of the small hole, making the stress concentration much more localised. For the large hole, a larger volume of material is subjected to high stresses, leading to higher probability of containing a flaw. Strength prediction methods based on boundary stresses are simple to use but do not account for the localised material response near the hole. As a result, these methods underestimate the strength of the laminates.

Two-parameter methods

In order to account for the localised damage prior to failure previously described, two-parameter methods were applied. These methods are based on the Whitney–Nuismer[44] failure criterion for unloaded holes and the parameters considered are the unnotched tensile strength and a characteristic dimension. Two approaches were proposed, the point stress and the average stress methods. In the first method it was assumed that failure occurs when the direct stress in the direction of the load at a distance d_{0t} away from the hole, measured in the net-tension plane, is equal to or greater than the strength of the unnotched material. The second method considered that failure occurs when the average stress over some distance a_{0t} equals the unnotched material strength. These distances were considered a material property. These criteria were formulated for the case of uniaxial tension where combined stresses play an inconsequential role in the failure process. In cases where this cannot be assumed, these criteria must be recast.

In later investigations, Nuismer and Labor[45,46] applied the average stress method to predict the strength of unloaded holes in tension[45] and of both unloaded and loaded holes in

compression[46]. The characteristic distance was now considered to be dependent upon laminate quality and type of load. Higher quality laminates have smaller values of a_{0t}. The predicted strengths for the tension case showed good agreement with experimental results. The value of the characteristic distance for compression was found to be larger than for tension. Good agreement between experimental and predicted compressive strengths was found only for laminates with unloaded holes.

In order to predict failure modes, Agarwal[47] proposed some modifications to the average stress criterion. The contact angle between the rigid bolt and the laminate was assumed to be 180° and the NASTRAN finite element software was used in a frictionless analysis. The unnotched laminate strength was determined through the use of the maximum strain theory. To predict tension failure, the stresses normal to the radial direction are averaged over a distance a_{0t} along the lines AB represented in *Figure 12*. When the averaged stress over a distance a_{0t} along AB, A"B′ and A"B" reaches the laminate tensile strength in the direction tangential to the point on the hole circumference under consideration, tension failure is assumed to occur. The distance a_{0t} was assumed to be 0.299 cm. The same procedure is applied to the radial stresses over a_{0c} along CD, C"D′ and C"D" to predict bearing failure. The computed average stresses are compared with the laminate compressive strength along the same line. The distance a_{0c} was considered to be 0.622 cm. When the average shear stress along EF reaches the shear strength of the laminate, shear-out failure is assumed to occur. The distance a_{0s} was assumed to be 1.143 cm for end distances greater than this value, and equal to the end distance in other cases. It was concluded that the predicted failure loads were quite sensitive to the values of the characteristic distances. Experimental tests were conducted and the failure modes were successfully predicted. The accuracy of the predicted strengths was dependent upon the laminate configuration. The largest differences occurred in the $(\pm 45°)_{2s}$ and $(0°/90°)_{2s}$ laminates, where the non-linear behaviour previously described[28] was not modelled, and were, respectively, 49% and 41%.

Wilson and Pipes[48] used the point stress criterion to study the influence of both *e/d* and *w/d* ratios on the shear strength of loaded holes. The shear stress distribution in the shear-out plane was obtained by a finite element model and then fitted to a curve using a polynomial expression. A 180° contact angle and a frictionless contact were assumed. The ratios *w/d* and *e/d* were then varied and plots relating the maximum shear stress with these ratios were obtained. This procedure allowed the definition of parameters that are functions of *w/d* and *e/d* and the inclusion of these parameters in the representation of the stress profile. The characteristic distance d_{0s} was assumed to be a function of the hole size:

$$d_{0s} = \frac{1}{c}\left(\frac{R}{R_0}\right)^m \tag{7}$$

where R is the hole radius, R_0 a reference radius and c and m two parameters obtained by measuring the notched and unnotched laminate shear strengths for two fastener sizes. For a $(45°/0°/-45°/0°_2/90°)_s$ laminate, very good agreement was found between predicted shear strength and experimental results obtained for three fastener sizes. It should be noticed that this result can be partially due to the fact that two of the fastener sizes considered were used to obtain c and m. It was predicted that the shear stress concentration decreases with increasing *w/d* and increases with increasing *e/d*.

A similar procedure was adopted by York *et al.*[49] to investigate tension failures in bolted joints. As the effect of *e/d* on the net tension stress profile was found to be negligible, only the effect of *w/d* on the tension strength was investigated. The tensile stress concentration factor was found to decrease with increasing *w/d* values. Using the same laminate configuration, strength predictions were compared with experimental data and, as before, good agreement was achieved. These procedures have the drawback of being unable to predict the failure modes. In order to predict the laminate strength, the modes have to be known a priori and, for several lay-ups and laminate geometries, this is not straightforward.

Combined methods

Several methods have been proposed that consist of combining the concepts of the Whitney–Nuismer characteristic distance[44] and a failure theory. Chang *et al.*[50] used a two-dimensional finite element model, assuming a frictionless contact, a rigid pin and a cosine normal load distribution in the pin-hole boundary. The Yamada–Sun[51] failure criterion was then applied together with a proposed characteristic curve. The Yamada–Sun[51] failure criterion is based on the assumptions that just prior to failure very ply has failed due to cracks along the fibres, and that the shear strength of the symmetric cross-ply laminate, with the same number of plies as the laminate under consideration, represents the substantially higher shear strength of a lamina when it is in a laminate. This criterion has the form:

$$\left(\frac{\sigma_{11}}{X}\right)^2 + \left(\frac{\sigma_{12}}{S_c}\right)^2 = e_f^2 \tag{8}$$

where σ_{11} and σ_{12} are respectively the longitudinal and shear stress in a ply, X is the ply longitudinal strength and S_c the ply shear strength measured from a cross-ply laminate.

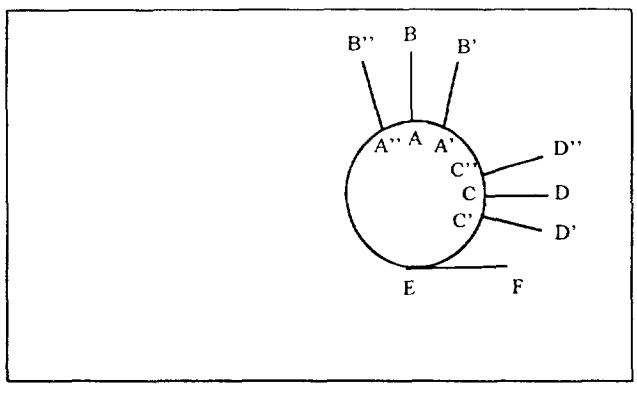

Figure 12 Definition of characteristic lengths[47]

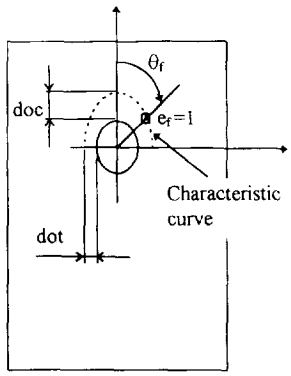

Figure 13 Characteristic curve[50]

When e_f is equal to, or higher than 1, in a ply, laminate failure is assumed to occur. The characteristic curve was assumed to depend only on the material and is defined by

$$r_c(\theta) = d/2 + d_{0t} + (d_{0c} + d_{0t})\cos\,\theta.$$

d_{0t} and d_{0c} are the characteristic dimensions for tension and compression, respectively. These parameters were obtained experimentally by measuring the tensile and compressive strength of notched laminates. The form of the characteristic curve is represented in *Figure 13*. The location on the characteristic curve where e_f first reached 1, θ_f, allows the definition of the failure mode. For $-15° \leq \theta_f \leq +15°$ failure occurs in the bearing mode, for $+30° \leq \theta_f \leq 60°$ in the shear-out mode and for $+75° \leq \theta_f \leq +90°$ in the tension mode. The results were compared with experimental results obtained by Agarwal[47] and in most cases the results agree with the data to within about 10%. As expected, the best results were obtained for the quasi-isotropic laminate, where the assumption of a cosine normal load distribution is acceptable. It should be noticed that the results are quite sensitive to the values of the characteristic distances and that for laminates with a large proportion of 0° fibres the results are sensitive to the value of S_c. Due to the fact that the transverse direct stress, σ_{22}, in the Yamada–Sun[51] failure criterion was assumed to be zero, this approach is not suitable when the transverse strength of the lamina, Y, governs the ultimate failure of the laminate.

Investigations based on this procedure were performed by several authors[52–54]. Murthy *et al.*[52] used an inverse technique where a rigid pin and a frictionless contact were assumed and the contact arc and pin-hole stress distributions were calculated rather than assumed. The authors concluded that for a $(0°/90°_5)_s$ GRP laminate the assumption of the cosine distribution leads to underestimation of bearing failure and overestimation of shear and tensile loads.

Eriksson[53] using the two-dimensional finite element model previously described[20] applied the point stress criterion to predict tension failure. It was assumed that failure initiation occurs at points on the hole boundary where fibres are either tangential or normal to the boundary. The characteristic distance should be calculated at each one of these points. The concept of a characteristic curve together with the Yamada–Sun[51] failure criterion was used to predict bearing failure. The author considered that bearing failures initiate in the interval $-45° \leq \theta \leq +45°$. The shapes of the characteristic curves obtained are strongly dependent on lay-up. No comparison with experimental results was made and the shear-out failure was not predicted. As the tension failure generally occurs in one defined plane the points were the characteristic distances are determined could have been limited.

Lin and Lin[54] used the direct boundary element method to determine the stress distribution around a loaded hole. A rigid pin and a frictionless contact were assumed at the pin-hole boundary and the effect of end distance on the strength of $(0°_2 / \pm 45°/90°)_s$, $(0°_2 / \pm 45°)_s$ and $(0°/90°)_{2s}$ laminates was investigated. Chang's[50] concept of a characteristic curve was used and it was concluded that the maximum strength decreases when *e/d* decreases. Qualitatively, this result is in agreement with experimental results[2].

A different approach was used by Arnold *et al.*[55]. From experimental tests made on pinned and clamped joints and from a finite element model the points at the net-tension and bearing planes, where the Hoffman and maximum stress failure criteria were first satisfied, were determined. The maximum value and corresponding position of these criteria around the hole boundary were also determined, and three characteristic lengths were then obtained. For a given laminate and type of joint (pinned or clamped) this procedure allows the prediction of strength and failure modes for other geometries. For GFRP, good agreement between predictions and experimental results was obtained using the Hoffman failure criterion. Only the net-tension and bearing modes of failure can be predicted using this method. Since all joints failed in the net-tension mode further analyses are required to verify the accuracy of this procedure to predict the bearing mode of failure.

The non-linear shear stress–shear strain behaviour was considered by Chang *et al.*[56]. The analysis follows that proposed in a previous work[50], including the non-linear shear stress–shear strain relation in the Yamada–Sun[51] failure criterion. The relation used was the one proposed by Hahn and Tsai[57]:

$$\gamma_{xy} = \left(\frac{1}{G_{xy}}\right)\sigma_{xy} + \alpha_1 \sigma_{xy}^3 \qquad (9)$$

α_1 being an experimentally determined constant. For cross-ply and angle-ply laminates the strength predictions using this method were more accurate than in the previous model[50] whilst for other laminate configurations the linear and non-linear predictions were in very close agreement. As in Sarabian's investigation[28], the current results highlight the importance of including the non-linear relation in the analysis of cross-ply and angle-ply laminates.

Fracture mechanics methods

These methods are generally based on linear elastic fracture mechanics (LEFM) and were developed for both unloaded[58,59] and loaded holes[60,61]. In the case of unloaded holes investigations were made for traction[58] and compression[59] loading. A damage zone model was considered, where damage around the hole is represented by an equivalent crack with cohesive forces acting at the crack surfaces. This crack

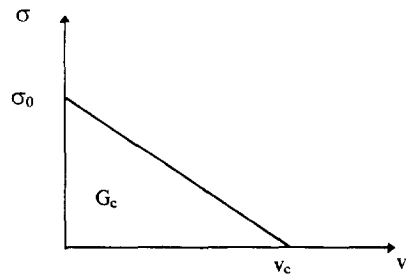

Figure 14 Relation between cohesive stress and crack opening[58]

represents matrix cracking and delamination in the traction case[58], and micro-buckling and delamination in the compression case[59]. A linearly decreasing relation between the cohesive stress and the crack opening, v, was assumed, representing the increase in the extent of damage with increasing load, and the stress at the crack tip was assumed equal to the unnotched laminate strength, as shown in *Figure 14*. The area under the curve is the total fracture energy developed in the damage zone, G_c. To predict notched strength the unnotched to notched strength obtained in experimental tests versus the fracture energy relation was determined using a two-dimensional finite element method, and the results were plotted versus the fracture energy. For one given crack length, the value of G_c which gives the fracture load equal to the experimental result is chosen. This value is considered a material constant for a certain lay-up.

Eisenmann[60] used a different concept to predict the strength of loaded holes. The approach consists of comparing the experimentally determined laminate fracture toughness with values of the mode I stress intensity factor, K_I, at eight locations on the hole boundary where cracks are assumed to occur. The values of laminate strength and fracture toughness at these locations are measured using tensile coupons and edge-notched specimens. These specimens represent the laminate properties in the direction tangential to the point at the hole boundary under consideration. The lengths of the cracks are obtained using this value and K_I is calculated using the boundary integral equation at each of the crack locations considering five basic load conditions. Failure is assumed to occur when K_I is equal to the fracture toughness. For a $(0^\circ_2 / \pm 45^\circ)_s$ GFRP laminate very good correlation with experimental results was obtained. The correlation between the failure location and failure mode was not made.

Schultz *et al.*[61] considered a pseudo-crack, which is related to the physical cracking of the laminate, to predict tension failure of a loaded hole. Assuming a cosine distribution and a contact angle of 180° a two-dimensional finite element model was created to determine the stress intensity factors in both mode I and II, K_I and K_{II}. The failure criterion used is an extension of the maximum principal stress criterion used for brittle isotropic materials and assumes that crack extension occurs in the direction along which the circumferential stress $\sigma_{\theta\theta}$ is maximum and the shear stress $\sigma_{r\theta}$ is zero. Failure is assumed to occur when the circumferential stress at the tip of the pseudo-crack is equal to or greater than the critical circumferential stress for a specific orientation. This critical value is determined experimentally from critical values of the fracture toughness. Good agreement between experimental and predicted results was achieved for a $(0^\circ/ \pm 45^\circ/0^\circ/90^\circ/0^\circ/ \pm 45^\circ/0^\circ/ \pm 45^\circ/0^\circ)_s$ CFRP laminate. Not such good agreement was found for a $(0^\circ/ \pm 45^\circ_2 /90^\circ/ \pm 45^\circ_3 /0^\circ)_s$ CFRP laminate. This effect can be related to the failure criterion used, which was developed initially for isotropic materials. In the case of the second laminate the high percentage of $\pm 45^\circ$ plies can lead to non-linear behaviour[28]. Further development is required to predict other modes of failure and to apply this procedure to other lay-ups.

Progressive damage methods

Progressive damage models were developed to deal with the damage that occurs prior to laminate failure in a more direct manner than the techniques previously discussed. These models try to simulate damage initiation and growth, using elastic property degradation models that are usually a function of the type of damage that occurred. Models were developed for both unloaded[62–66] and loaded[67–71] holes.

Chang and Chang[62] developed a progressive damage model for notched laminates subjected to tensile loading that was later modified to predict tension and shear-out failures at loaded holes[67]. In contrast to previous work[50,56], the authors considered that a two-dimensional model was unsuitable for predicting bearing failure since the failure mechanisms of this failure mode are three-dimensional and involve fibre buckling, fibre-matrix crushing and volume expansion. A finite element model was created where the contact problem was considered and a frictionless contact assumed. Both geometric and material non-linearity were considered. The non-linear relation between the shear stress and shear strain was previously defined[56]. Four different failure mechanisms were considered, namely matrix cracking, fibre-matrix shear-out, fibre breakage and matrix compressive failure. Matrix cracking was predicted using the Yamada–Sun failure criterion[51], taking into account the expression (9), resulting in:

$$\left(\frac{\sigma_{22}}{Y}\right)^2 + \frac{\dfrac{\sigma_{12}^2}{2G_{12}} + \dfrac{3\alpha_1\sigma_{12}^4}{4}}{\dfrac{S_c^2}{2G_{12}} + \dfrac{3\alpha_1 S_c^4}{4}} = e_f^2 \qquad (10)$$

where Y is the transverse tensile strength of a ply. When at one position in any of the plies in a laminate e_f is equal to or greater than 1, matrix cracking is assumed to occur in that position and layer. It should be noticed that in previous investigations[50], these authors assumed that the laminate failed when the criterion was satisfied in any layer, whilst in the present work only the zone in the layer where the criterion is satisfied is assumed to fail. Both fibre–matrix shear-out failure and fibre breakage were predicted using the Yamada–Sun[51] criterion:

$$\left(\frac{\sigma_{11}}{X}\right)^2 + \frac{\dfrac{\sigma_{12}^2}{2G_{12}} + \dfrac{3\alpha_1\sigma_{12}^4}{4}}{\dfrac{S_c^2}{2G_{12}} + \dfrac{3\alpha_1 S_c^4}{4}} = e_f^2 \qquad (11)$$

where X is the longitudinal strength of a ply. Compressive failure was predicted using the Hashin failure criterion[71]:

$$\left[\left(\frac{Y_c}{2S_c}\right)^2 - 1\right]\frac{\sigma_{22}}{Y_c} + \left(\frac{\sigma_{22}}{2S_c}\right)^2 + \frac{\dfrac{\sigma_{12}^2}{2G_{12}} + \dfrac{2\alpha_1\sigma_{12}^4}{4}}{\dfrac{S_c^2}{2G_{12}} + \dfrac{3\alpha_1 S_c^4}{4}} = e_f^2 \tag{12}$$

Once failure occurs, material properties in the damage areas degenerate. The degrees of property loss are dependent on the failure mechanism. When matrix cracking or compressive matrix failure occurred it was assumed that the transverse modulus E_{22} and Poisson's ratio ν_{21} were reduced to zero. In the case of the fibre-matrix shear-out and fibre breakage, both E_{22} and ν_{21} are reduced to zero but the longitudinal modulus E_{11} and the shear modulus G_{12} of the failed zone degenerate according to a Weibull distribution as follows:

$$\frac{E_{11}^d}{E_{11}} = \exp\left[-\left(\frac{A}{\delta^2}\right)^{\beta_1}\right] \tag{13}$$

$$\frac{G_{12}^d}{G_{12}} = \exp\left[-\left(\frac{A}{\delta^2}\right)^{\beta_1}\right] \tag{14}$$

These expressions are based on the micro-mechanics approach for fibre bundle failure[72] assuming that the property reduction distribution has the same shape as the fibre strength reduction distribution. E_{11}^d and G_{12}^d are the reduced moduli, δ is the fibre failure interaction zone[72], A is the damage zone predicted by the failure criterion and β_1 is the shape of the Weibull distribution for the property degradation. For CFRP, δ was calculated to be 0.00127 mm and β_1 was assumed[72] to be 7.6. Once damage propagated across the laminate, total failure was assumed to occur. For a large number of laminate configurations and geometries, calculated failure strengths agreed with experimental results within 20% for most cases, and the failure modes were accurately predicted by analysing the damage propagation in the laminate. No improvement in the accuracy of the predicted strengths was found when comparing the present results with results from previous investigations made by the same authors[50,56]. An interesting feature of this model is the possibility of seeing the propagation of the damage in the laminate for the different lay-ups. Using this model the previously described limitation of the Yamada–Sun failure criterion is annulled. In order to use this approach with other materials several parameters that are not easily determined (β_1,δ) should be known.

This approach was later modified by Chang and Lessard[63] and Chang *et al.*[64] to predict the strength of unloaded holes in compression and tension, respectively. The failure criterion for matrix compressive failure and the property degradation model for the fibre-matrix shear-out were modified. The longitudinal modulus is now unaffected by the fibre-matrix shear-out. The effect of ply clustering on the reduction of ply transverse and shear strength was considered using expressions for these parameters that are functions of the degree of ply clustering. For several lay-ups of CFRP comparisons were made with experiment results and the predicted damage patterns were basically consistent with X-radiographs and photographs of damaged specimens. The predicted size of internal damage was more extensive in clustered laminates. The predicted failure loads were in good agreement with experimental results. However, these results can be partially due to the fact that the value of δ used was the one in the interval calculated for CFRP that best fit with the test data. The damage growth on the compression model[63] was sensitive to the finite element mesh used, so the authors adopted meshes in order to obtain the expected damage propagation for each lay-up. This procedure disables the generalisation of the model for lay-ups and geometries in which damage progression is difficult to predict. One of the main effects of ply clustering was considered by Hart–Smith[73] to be delamination. The effect of delamination was not investigated in this analysis and can only be dealt with by a three-dimensional model. Further development is required to apply these approaches to loaded holes.

In contrast to the approach defined by Chang[62], Tan[65] assumed that the stiffness degradation of a lamina does not depend on how the damage is caused. For a laminate with an unloaded hole and for tension loading, fibre failure was predicted by a proposed quadratic criterion which utilises the longitudinal tensile and compressive strength of a lamina and the lamina direct stress in the fibre direction. Matrix cracking was predicted by the Tsai–Wu[74] criterion. The stiffness degradation was represented by factors assumed to be material properties which represent the damage state of the lamina. E_{11}, E_{22} and G_{12} were reduced by the product of its initial value with a corresponding factor. Total failure was assumed to occur when fibres across the entire width of a ply are broken or when substantial matrix failure has occured in all the laminate. For CFRP laminates with several lay-ups predictions correlate closely with experimental strengths. Damage progression basically agreed with experimental results obtained by X-radiographic examination of the specimen at several load levels. It should be noticed that the results were very sensitive to the values of the degradation factors assumed and the consideration of subtantial matrix failure is not specific enough to predict total failure.

The effects of temperature on the strength of pin-loaded laminates were investigated by Chen and Lee[68]. A frictionless contact was assumed and the Hashin[71] failure criterion was used to predict fibre breakage and matrix cracking. When fibre failure occurred E_{11}, ν_{12}, ν_{21} and G_{12} become zero, and when matrix cracking occurred E_{22}, ν_{12}, ν_{21} and G_{12} become zero. It was assumed that an element fails when all of the laminae in the element fail. The predicted strengths for a $(0°/45°/90°/-45°)_s$ GFRP laminate at 20°C, 40°C, 60°C, 80°C, 100°C and 120°C were within 2% (at 40°C) and 55% (at 80°C) of experimental data. It was concluded that there is a gradual reduction of the strength with increasing temperature and that strength decreases rapidly when the temperature exceeds the softening point of the resin. The type of failure also depends on the temperature. Under room temperature

failure started by matrix cracking and developed gradually to fibre breakage that finally results in failure. At elevated temperatures, due to the softening of the matrix, the failure initiated by fibre breakage and the propagation of this type of failure lead to total failure. The geometric effects (*e/d* and *w/d*) on the strength were less significant at high temperatures. This model was also applied to CFRP laminates and it was concluded that the effect of temperature on the strength was not significant for temperatures lower than the softening point of the matrix. When the temperature exceeded this value a strength reduction of approximately 50% was found. In contrast to GFRP, the geometric effects were not significantly affected by temperature. The temperature effect on damage propagation was not as significant as in the case of GFRP. Although it was shown using photos that the damage zone in one GFRP specimen is a function of the temperature, the results described were not verified experimentally.

Tsujimoto and Wilson[75], assuming a cosine load distribution and a rigid pin, used a two-dimensional elasto-plastic finite element model which included the effects of friction and non-linear shear stress–shear strain behaviour. An elastic–perfectly plastic constitutive equation coupled with the Hill yield criterion for orthotropic materials was used. The modes of failure were defined by the position at the hole boundary where failure occurred. For a $(0°_6/\pm 45°_2/90°)_s$ laminate reasonable agreement between experimental and predicted strengths was found for bearing and shear-out failure modes. However, net-tension failures were not accurately predicted. This mode of failure was relatively insensitive to friction effects, whilst with increasing friction shear-out and bearing strengths increased. Such a result for the bearing strength is not surprising since it was shown[12] that the radial stress near $\theta = 0°$ decreases with increasing friction. The assumption of cosinusoidal load distribution prevents the application of this model to other lay-ups.

Lessard and Shokrieh[69] used two-dimensional linear and non-linear models to predict the strengths of pin-loaded holes. In the linear model five types of failure were considered. Matrix tensile and compressive failure, fibre-matrix shearing and fibre tensile failure were predicted using the Hashin[71] failure criterion. A criterion with the form:

$$\left(\frac{\sigma^2_{11}}{X_c}\right) \geq 1, \ \sigma_{11} \geq 0 \qquad (15)$$

where X_c is the longitudinal compressive strength was suggested to predict fibre compressive failure. When matrix compressive or tensile failure occurred ν_{21} and E_{22} in the zone and ply where the criterion was satisfied become zero. For fibre-matrix shearing ν_{12}, ν_{21} and G_{12} become zero and for fibre tensile and compressive failure all the elastic constants were assumed to be zero. For several values of *e/d* and *w/d* of a $(0°/\pm 45°/90°)_s$ CFRP laminate the linear model was capable of predicting the failure load with satisfactory accuracy, and captured the shear-out and net-tension failure modes. The geometric and material non-linear model was based on the previous work performed by Chang and Lessard[63], applying equation (15) to predict fibre compression failure. However, the property degradation model associated with this type of failure was developed to avoid numerical problems. As occurred with the linear model, final failure was predicted within 20% of experimental results. This model was more accurate at predicting the bearing mode of failure. This effect can be related to the consideration of geometric non-linearity in this model.

In a previously described investigation Chen *et al.*[26] developed a three-dimensional model capable of predicting delamination onset, based on the Ye[76] delamination criterion. Ye[76] assumes that, regardless of the nature of loading, edge delamination is driven by the interlaminar stresses that exist near the laminate free edges. The criterion proposed is based on the work of Hashin and Rotem[77] and has the form:

$$\left(\frac{\sigma_{33}}{Z}\right)^2 + \left(\frac{\sigma_{31}}{G_{31}}\right)^2 + \left(\frac{\sigma_{23}}{G_{23}}\right)^2 \geq 1, \ \sigma_{33} \geq 0 \qquad (16)$$

or

$$\left(\frac{\sigma_{31}}{G_{31}}\right)^2 + \left(\frac{\sigma_{23}}{G_{23}}\right)^2 \geq 1, \ \sigma_{33} \leq 0 \qquad (17)$$

Since the strength properties are valid over a finite material volume, the stress components should be calculated at a distance from the free edge. Ye[76] assumed this distance equal to two ply thickness. For $(0°_6/90°_6)_s$ and $(90°_6/0°_6)_s$ laminates it was concluded that increasing friction decreased the delamination onset region at the bearing plane, but enlarged the delamination onset region along the other zones of contact. Different delamination onset zones were obtained for different stacking sequences.

This model was developed by Chen and Lee[70] to investigate bolted joints under bending loads. Simply supported laminates with a bolt at the centre and a vertical load applied at that location were studied. $(0°_8/90°_8)_s$ and $(90°_8/0°_8)_s$ CFRP laminates were investigated and brick elements with 8 layers having the same fibre orientation in each element were used. The maximum stress theory was used to predict fibre breakage, matrix cracking and fibre-matrix shearing. The Ye[76] criterion was used to predict delamination onset. The complete ply failure approach was used, so if any of the failure criteria were satisfied at one layer of an element this element was assumed to have failed. The elastic properties of such an element were then reduced to zero. Good agreement between the computed and the experimental strengths was found, however no comparison was made concerning damage propagation. Further development is required to apply this model to joints with in-plane loads, taking into consideration that the maximum stress failure criterion is not accurate when multiaxial stresses are present[78], as for loaded holes of joints with in-plane loads.

Gamble *et al.*[66] used ABAQUS software to create a three-dimensional model of a plate with an unloaded hole using stacked brick elements, i.e., each element represents part of one layer. The failure criterion selected was a modified form of the Hill criterion that was able to predict fibre failure, matrix splitting and delamination within a single ply.

Delamination between layers was predicted by applying these criteria to thin resin-rich layers that were modelled between each layer. These resin-rich layers were assumed to have the moduli and the failure strength of the cured resin. In-plane failure of these layers represented interlaminar delamination. The material degradation was a function of the type of failure. When fibre failure occurred E_{11}, G_{12}, ν_{12} and ν_{13} became zero in the elements where the criterion is satisfied. In the case of delamination in a ply E_{33}, G_{13}, G_{23}, ν_{31} and ν_{32} become zero. For a $(0°/90°)_s$ CFRP laminate the predicted and measured failure loads agreed within 5%. Although the progression of damage was not verified experimentally, delamination occurred near the net-tension plane. This result is in agreement with the hole size effect observed experimentally[1]. Matrix delamination within a single ply is not the usual type of failure. As the resin-rich layers have isotropic behaviour a different failure criterion could have been used to predict inter-ply delamination.

Application to multi-fastener joints

The strength prediction methods previously described have been applied to predict the strength of joints with several loaded holes.

Agarwal[79] used an experimental and analytical model to predict the strength of joints with several configurations. Specimens were instrumented with strain gauges to determine the load distribution in the joint and experimental results were obtained for a $(0°_2 / \pm 45°/0°_2 /90°/0°)_{2s}$ CFRP laminate. Assuming that fasteners in a single row share the load equally, the previously described methodology[47] to predict single hole strength was then applied to predict the failure load and failure mode of the multi-row joints. It was concluded that almost all the joints failed in the net-tension mode. For the same number of bolts in a line, the ratio of gross area failure stress to unnotched failure stress was found to be slightly higher in the joints with fewer bolts in a row. This result is in agreement with the predictions of Hart-Smith[1]. The accuracy of the predicted strengths depended on the number of fasteners in a row. In joints with 2 fasteners in a row, predictions agreed within 10% with experimental results, whilst in joints with 3 bolts in a row the agreement was within 24%. These results can be related to the assumption of an equal load distribution in one row of fasteners, whereas, in fact, it has been shown[34] that this assumption is a poor approximation. The fact that the interaction between stress distributions around each hole was not modelled could have some importance in these results.

Chang *et al.*[80] used their previous model[50] to predict the strength of joints with two bolts in a row or two bolts in a line. In contrast to the previous work[50], it was assumed that the characteristic distances were functions not only of the material but also of the geometry. The difference between predicted and experimental strengths varied from 10 to 40% and the failure modes were accurately predicted.

Considering two holes in a line, Hyer and Chastain[81] addressed the problem of adjusting the proportion of load transmitted at each hole in order to obtain maximum joint strength. A cosinusoidal load distribution at the pin-hole boundary and a contact angle of 180° were assumed. The characteristic curve defined by Chang[50] and the Yamada–Sun[51] failure criterion were used to predict failure. It was concluded that in almost all cases a load proportioning of 50% at each hole does not result in maximum joint strength. The optimum value depends on material, lay-up and joint geometry, but the strength obtained was not substantially different from the joint strength for a load proportioning of 50%.

A comprehensive experimental and numerical investigation on the effects of the bearing stress to by-pass stress ratio, β was performed by Naik and Crews[41,42]. This ratio was previously defined[35] by the expressions (4)–(6). β was

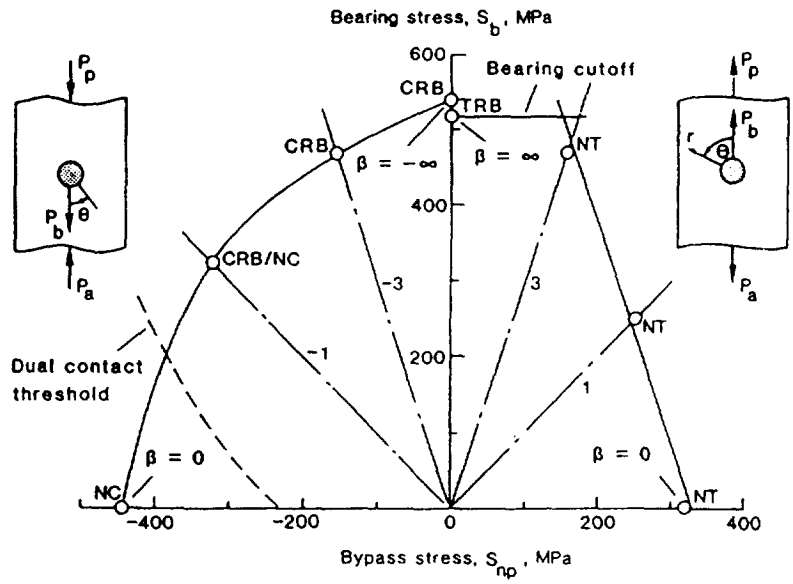

Figure 15 Bearing-by-pass diagram for damage onset stress[42]

assumed to depend on the joint stiffness and configuration. Assuming that one fastener in a multi-fastener joint can be represented by a single fastener coupon subjected to both bearing and by-pass loads, an experimental test system that could simultaneously apply these loads was used. This system consisted of two hydraulic actuators that independently load the ends of the specimen, making possible the application of a constant value of β until damage onset occurs. The damage onset was detected by the first non-linearity in the load–displacement curve. The bearing-by-pass diagram obtained for a $(0°/45°/90°/-45°)_{2s}$ CFRP laminate is shown in *Figure 15*. The symbols (○) represent measured S_b and S_{np} values for damage onset, and NT, TRB, NC and CRB mean respectively net section tension, tension reacted bearing, net section compression and compression reacted bearing. It can be seen that the tension case with net-tension damage can be represented by a straight line. It was concluded that local stresses responsible for damage onset consist of a component due to bearing and a second superimposed component due to by-pass loading. The failure envelope obtained is similar to the one obtained by Hart–Smith[4]. It should be noticed that for compressive loading the damage for the filled hole case ($S_{np} = 0$) initiated at a higher stress than for the open hole case ($S_b = 0$). This fact was due to the dual bolt-hole contact that occurred in the filled hole case, allowing load transfer across the hole. For all by-passing loading ($\beta = 0$) the specimens failed soon after damage onset, whilst for all bearing load ($\beta = \pm\infty$) the specimens failed at considerably higher loads than the damage onset load. The net-tension ($S_b = 0$), tension reacted bearing ($S_{np} = 0$) and net-compression ($S_b = 0$) damage onset modes were analysed using X-radiographs and micrographs of the specimens. For the net tension mode damage occurred by matrix cracking, in the 90° and ± 45° plies, and delamination and fibre failures in the 0° ply, near $\theta = 90°$. The fibre failure apparently followed the direction of matrix cracking in the adjacent 45° ply. For tension reacted bearing, damage appeared to be concentrated near the outer surface plies. Matrix cracking occurred in the 0°/45° and 45°/90° interfaces, fibre failures associated with transverse cracking were visible in the 90° plies near $\theta = 0°$ and fibre crushing occurred in the 0° plies, near $\theta = 0°$. In the case of net-compression damage delamination occurred at a lower level than in the bearing damage. Matrix cracking and fibre failure occurred in the ± 45° plies and compressive fibre failure with evidence of micro-buckling was visible in the 0° plies. Using the previously described inverse technique[21], the NASTRAN finite element code was used to determine lamina strains[41] and stresses[42] around the hole boundary. The bearing and by-pass stresses applied to the model corresponded to the experimentally determined damage onset stresses for the modes previously investigated. In almost all cases the strains and stresses around the hole boundary were greater than the unnotched ultimate strains and stresses. As previously discussed, these differences are typical of methods based on hole stress or strain distributions used together with failure theories. As damage onset was found to be governed by fibre failure, in order to predict strength it was assumed that damage onset occurs when the peak ϵ_{11} in a ply reaches the experimentally determined critical value for each failure mode. Using such procedures the calculated damage onset stresses and failure modes for several values of β agreed reasonably well with experimental results. However, the accuracy was dependent on β and for compressive loading unconservative predictions can occur.

CONCLUSIONS

From the analysis of previous investigations on the behaviour of mechanically fastened joints we can conclude that there are some unresolved issues.

The models to determine the stress distribution around a pin-loaded hole should take into account the effects of friction, clearance or interference and the contact area should be calculated instead of being assumed. Although several investigations were made concerning the effects of friction on the stress distribution around a pin-loaded hole, there are insufficient studies of the effect of friction on joint strength. Investigations regarding the effect of interference between the pin and the hole on the joint strength were not found in the literature. Although the use of mechanically fastened joints in cross-ply and angle-ply laminates is not recommended, in the analysis of such laminates the non-linear shear stress-shear strain relation should be considered.

There is no definitive method to predict joint strength. Although some of the methods described achieved good results for some laminate configurations and failure modes, extrapolation to other situations is not always possible. Methods based on boundary stresses and failure theories underestimate the joint strength. Fracture mechanics methods require the determination of complex material properties and assume plane stress conditions at the hole boundary, where three-dimensional stresses are present. The accuracy of two-parameter methods is dependent on experimentally determined values that should be determined for each material and lay-up. Both fracture mechanics and two-parameter methods take into account the stress concentration relief prior to failure but are only able to predict ultimate strength. Progressive damage methods have the advantages of being able to determine failure mechanisms, the direction of failure propagation, failure mode and both ultimate and residual strengths. However, the models developed are based on two-dimensional models, meaning that only two-dimensional failure mechanisms that contribute to the stress concentration relief prior to failure are considered. One of the main causes that leads to such relief is delamination and this kind of damage can be accurately modelled using three-dimensional models. These models also apply two-dimensional failure criteria at the hole boundary where three-dimensional stresses are present. It is now of general agreement that the bearing mode of failure is governed by three-dimensional effects, which means that three-dimensional models are more appropriate to predict this mode of failure. The experimental results highlighted the importance of stacking

sequence and lateral constraint on the joint strength. These effects should be taken into account using three-dimensional models. Considering these facts, we can conclude that a three-dimensional model is required to accurately predict the strength of mechanically fastened joints. Some investigations concerning the determination of the stress distributions around a pin-loaded hole using three-dimensional models have been made. However, investigations concerning the prediction of strength of mechanically fastened joints using three-dimensional models were not found in the literature.

There is no general agreement about the failure modes that should be used in the progressive damage methods. Some authors considered the degradation of properties as a function of the type of failure whilst others considered that the two parameters were independent. Concerning the property degradation models, some approaches considered that the elastic properties are reduced to zero in the damage zones, whilst other models assumed a gradual reduction of elastic properties in those zones. The application of a property degradation approach to a three-dimensional model requires a sensible three-dimensional failure criterion and a three-dimensional property degradation rule.

Generally, the investigations of multi-fastener joints assumed that there was no interference between the stress distributions at several holes. In situations where the holes are closer together it is important to develop models capable of predicting the joint strength taking into account stress distribution interference.

Experimental and analytical investigations on the behaviour of new advanced composite materials should be performed. The progressive damage models will have increasing importance in the investigation of tougher composites that can develop a significant amount of damage prior to failure. The good performance[1] of hybrid laminates (CFRP laminates with GFRP strips near the hole) was experimentally demonstrated but was not explained analytically. Recent experimental and analytical investigations on the behaviour of joints in GFRP pultrusions have been made[82–90], but further development is required to fully understand the characteristics of such joints and the influence of the complex fibre architecture present in pultruded components.

ACKNOWLEDGEMENTS

The first author wishes to acknowledge the support given by JNICT (Junta Nacional de Investigação Científica e Tecnol ógica), Portugal, Programa Ciência e Tecnologia do 2° Quadro Comunitário de Apoio.

REFERENCES

1. Hart-Smith, L.J., Mechanically-fastened joints for advanced composites—phenomelogical considerations and simple analysis. Douglas Paper 6748, 1978, 1–32.
2. Kretsis, G. and Matthews, F.L., The strength of bolted joints in glass fibre/epoxy lamiantes. *Composites*, 1985, **16**, 92–105.
3. Collings, T.A., The strength of bolted joints in multi-directional CFRP laminates. *Composites*, 1977, **8**, 43–54.
4. Hart-Smith, L.J., Design and analysis of bolted and riveted joints in fibrous composite structures. Douglas Paper 7739, 1986, 1-15.
5. Hodgkinson, J.M., de Beer, D.L. and Matthews, F.L., The strength of bolted joints in Kevlar RP. ESA SP-243, 1986, pp. 53–61.
6. Collings, T.A., On the bearing strengths of CFRP laminates. RAE Technical Report 82033, 1982, 1–23.
7. Matthews, F.L., Kilty, P.F. and Godwin, E.W., Load-carrying joints in fibre reinforced plastics. *Plastic and Rubber Process and Applications*, 1982, **2**, 19–25.
8. Quinn, W.J. and Matthews, F.L., The effect of stacking sequence on the pin-bearing strength in GFRP. *J. Compos. Mater.*, 1987, **11**, 139–145.
9. Muskhelishvili, N.I., *Some Basic Problems of the Mathematical Theory of Elasticity*. Noordhoff International Publishing, Leyden, The Netherlands, 1977.
10. Lekhnitskii, S.G., *Theory of Elasticity of an Anisotropic Body*. Holden Day, San Francisco, CA, 1963.
11. de Jong, T., Stresses around pin-loaded holes in elastically orthotropic or isotropic plates. *J. Compos. Mater.*, 1977, **11**, 313–331.
12. Zhang, K.D. and Ueng, C.E.S., Stresses around a pin-loaded hole in orthotropic plates. *J. Compos. Mater.*, 1987, **18**, 432–446.
13. Hyer, M.W. and Klang, E.C., Contact stresses in pin-loaded orthotropic plates. *Int. J. Solids and Structures*, 1985, **21**, 957–975.
14. Hyer, M.W., Klang, E.C. and Cooper, D.E., The effects of pin elasticity, clearance and friction on the stresses in a pin-loaded orthotropic plate. *J. Compos. Mater.*, 1987, **21**, 190–206.
15. de Jong, T., Stresses in pin loaded anisotropic plates. In *AGARD Conference Proceedings*, Vol. 427. AGARD, Madrid, Spain, 1987, pp. 5.1–5.17.
16. Conti, P., Influence of geometric parameters on the stress distribution around a pin-loaded hole in a composite laminate. *Compos. Sci. Technol.*, 1986, **25**, 1–19.
17. Wilkinson, T.L., Rowlands, R.E. and Cook, R.D., An incremental finite-element determination of stresses around loaded holes in wood plates. *Computers and Structures*, 1981, **14**, 123–128.
18. Rowlands, R.E., Rahman, M.U., Wilkinson, T.L. and Chiang, Y.I., Single and multiple-bolted joints in orthotropic materials. *Composites*, 1982, **13**, 273–279.
19. Crews, J.H., Hong, C.S. and Raju, I.S., Stress-concentration factors for finite orthotropic laminates with a pin-loaded hole. NASA Tech. Paper 1862, 1981, 1–40.
20. Eriksson, L.I., Contact stresses in bolted joints of composite laminates. *Composite Structures*, 1986. **6**, 57–75.
21. Naik, R.A. and Crews, J.H., Stress analysis method for a clearance—fit bolt under bearing conditions. *AIAA J.*, 1985, **24**, 1348–1353.
22. Ramamurthy, T.S., New studies on the effect of bearing loads in lugs with clearance fit pins. *Composite Structures*, 1989, **11**, 135–150.
23. Ramamurthy, T.S., Recent studies on the behaviour of interference fit pins in composite plates. *Composite Structures*, 1989, **13**, 81–99.
24. Agarwal, B.D. and Broutman, L.J., *Analysis and Performance of Fiber Composites*. John Wiley and Sons, New York, NY, 1990.
25. Matthews, F.L., Wong, C.M. and Chryssafitis, S., Stress distribution around a single bolt in fibre-reinforced plastic. *Composites*, 1982, **13**, 316–322.
26. Chen, W.H., Lee, S.S. and Yeh, J.T., Three-dimensional contact stress analysis of a composite laminate with bolted joint. *Composite Structures*, 1995, **30**, 287–297.
27. Smith, P.A., Pascoe, K.J., Polak, C. and Stround, D.O., The behaviour of single-lap bolted joints in CFRP laminates. *Composite Structures*, 1986, **6**, 41–55.
28. Sarabian, S.M., An experimental and finite element investigation into the nonlinear material behaviour of pin-loaded composite laminates. MTL Report TR 91-2, 1991, 1–265.
29. Barboni, R., Gandenzi, P. and Carlini, S., A three-dimensional analysis of edge effects in composite laminates with circular holes. *Composite Structures*, 1990, **15**, 115–136.
30. Marshall, I.H., Arnold, W.S. and Wood, J., Observations on bolted connections in composite structures. *Composite Structures*, 1989, **13**, 133–151.
31. Iarve, E., Stress analysis in laminated composites with fastener holes. In *Proceedings of the American Society for Composites 10th Technical Conference*. Technomic Publishing Co., Lancaster, PA, 1995, pp. 408–419.
32. Iarve, E., Spline variational three-dimensional stress analysis of

laminated composite plates with open holes. *Int. J. Solids and Structures*, 1996, **33**, 2095–2118.
33. Wang, S. and Han, Y., Finite element analysis for load distribution of multi-fastener joints. *J. Compos. Mater.*, 1988, **22**, 124–135.
34. Griffin, O.H., Hyer, M.W., Cohen, D., Shuart, M.J., Yalamanchili, S.R. and Prasad, C.B., Analysis of multifastener composite joints. *J. Spacecraft and Rockets*, 1994, **31**, 278–284.
35. Naik, R.A. and Crews, J.R., Stress analysis method for clearance-fit joints with bearing-by-pass load. *AIAA J.*, 1991, **29**, 89–95.
36. Kim, S.J. and Kim, J.H., Finite element analysis of laminated composites with contact constraint by extended interior penalty methods. *Int. J. Numerical Methods Engng*, 1993, **36**, 3421–3439.
37. Godwin, E.W. and Matthews, F.L., A review of the strength of joints in FRP—Part I: Mechanically fastened joints. *Composites*, 1982, **11**, 155–160.
38. Johnson, M. and Matthews, F.L., Determination of safety factors for use when designing bolted joints in GRP. *Composites*, 1979, **10**, 73–76.
39. Waszczak, J.P. and Cruse, T.A., Failure mode and strength prediction of anisotropic bolt bearing specimens. *J. Compos. Mater.*, 1971, **5**, 421–425.
40. Tang, S., Failure of composite joints under combined tension and bolt loads. *J. Compos. Mater.*, 1981, **15**, 329–335.
41. Naik, R.A. and Crews, J.H., Ply-level failure analysis of a graphite/epoxy laminate under bearing-bypass loading. NASA Tech. Memo. 100578, 1988, 1–35.
42. Crews, J.H. and Naik, R.A., Combined bearing-bypass loading on a graphite/epoxy laminate. *Composite Structures*, 1986, **6**, 21–40.
43. Crews, J.H., A survey of strength analysis methods for laminates with holes. *J. Aeronautical Society of India*, 1984, **36**, 287–303.
44. Whitney, J.M. and Nuismer, R.J., Stress fracture criteria for laminated composites containing stress concentrations. *J. Compos. Mater.*, 1974, **8**, 253–265.
45. Nuismer, R.J. and Labor, J.D., Applications of the average stress failure criterion: part I—tension. *J. Compos. Mater.*, 1979, **12**, 238–249.
46. Nuismer, R.J. and Labor, J.D., Applications of the average stress failure criterion: part II—compression. *J. Compos. Mater.*, 1979, **13**, 49–60.
47. Agarwal, B.L., Static strength prediction of bolted joint in composite materials. *AIAA J.*, 1980, **18**, 1371–1375.
48. Wilson, D.W. and Pipes, R.B., Analysis of the shearout failure mode in composite laminates. *1st International Conference on Composite Structures*. Applied Science Publishers, London, UK, 1981, pp. 34–49.
49. York, J.L., Wilson, D.W. and Pipes, R.B., Analysis of the net-tension failure mode in composite bolted joints. *J. Reinforced Plastics and Compos.*, 1982, **1**, 141–152.
50. Chang, F.K., Scott, R.A. and Springer, G.S., Strength of mechanically fastened composite joints. *J. Compos. Mater.*, 1982, **16**, 470–494.
51. Yamada, S.E. and Sun, C.T., Analysis of laminate strength and its distribution. *J. Compos. Mater.*, 1978, **12**, 275–284.
52. Murthy, A.V., Dattaguru, B., Narayana, H.L. and Rao, A.L., Stress and strength analysis of pin joints in laminated anisotropic plates. *Composite Structures*, 1991, **19**, 299–312.
53. Eriksson, I., An analysis method for bolted joints in primary composite. *AGARD Conference Proceedings 427*. AGARD, Madrid, Sapin, 1987, pp. 6.1–6.19.
54. Lin, C.C. and Lin, C.H., Stress and strength analysis of composite joints using direct boundary element method. *Composite Structures*, 1993, **25**, 209–215.
55. Arnold, W.S., Marshall, I.H. and Wood, J., Optimum design considerations for mechanically fastened composite joints. *Composite Structures*, 1990, **16**, 85–101.
56. Chang, F.K., Scott, R.A. and Springer, G.S., Failure strength of nonlinearly elastic composite laminates containing a pin loaded hole. *J. Compos. Mater.*, 1984, **18**, 464–477.
57. Hahn, H.T. and Tsai, S.W., Nonlinear elastic behaviour of unidirectional composite laminate. *J. Compos. Mater.*, 1973, **7**, 102–110.
58. Aronsson, C.G., Strength of carbon/epoxy laminates with countersunk hole. *Composite Structures*, 1995, **24**, 283–289.
59. Soutis, C., Curtis, P.T. and Fleck, N.A., Compressive failure of notched carbon fibre composites. *Proc. R. Soc. (London)*, 1993, **440**, 241–256.
60. Eisenmann, J.R., Bolted joint static strength model for composite materials. NASA Report TMX 3377, 1976, pp. 563–602.
61. Schulz, K.C., Packman, P. and Eisenmann, J.R., A tension-mode fracture model for bolted joints in composite laminates. *J. Compos. Mater.*, 1995, **29**, 37–58.
62. Chang, F.K. and Chang, K.Y., A progressive damage model for laminated composites containing stress concentrations. *J. Compos. Mater.*, 1987, **21**, 834–855.
63. Chang, F.K. and Lessard, L.B., Damage tolerance of laminated composites containing an open hole and subjected to compressive loadings: part I—analysis. *J. Compos. Mater.*, 1991, **25**, 2–43.
64. Chang, K.Y., Liu, S. and Chang, F.K., Damage tolerance of laminated composites containing an open hole and subjected to tensile loadings. *J. Compos. Mater.*, 1991, **25**, 274–301.
65. Tan, S.C., A progressive failure model for composite laminates containing openings. *J. Compos. Mater.*, 1991, **25**, 556–557.
66. Gamble, K., Pilling, M. and Wilson, A., An automated finite element analysis of the initiation and growth of damage in carbon-fibre composite materials. *Composite Structures*, 1995, **35**, 265–274.
67. Chang, F.K. and Chang, K.Y., Post-failure analysis of bolted composite joints in tension or shear-out mode failure. *J. Compos. Mater.*, 1987, **21**, 809–833.
68. Chen, W.H. and Lee, Y.J., Failure process and pin-bearing strength of laminated composites at elevated temperatures. *J. Plastics and Compos.*, 1992, **11**, 743–771.
69. Lessard, L.B. and Shokrieh, M.M., Two-dimensional modeling of composite pinned-joint failure. *J. Compos. Mater.*, 1995, **29**, 671–697.
70. Chen, W.H. and Lee, S.S., Numerical and experimental failure analysis of composite laminates with bolted joints under bending loads. *J. Compos. Mater.*, 1995, **29**, 15–36.
71. Hashin, Z., Failure criteria for unidirectional fiber composites. *J. Appl. Mech.*, 1980, **47**, 329–334.
72. Tsai, S.W. and Hahn, H.T., *Introduction to Composite Materials*. Technomic Publishing Company, Westport, 1980.
73. Hart-Smith, L.J., The role of biaxial stresses in discriminating between meaningful and illusory composite failure theories. *Composite Structures*, 1993, **25**, 3–20.
74. Tsai, S.W. and Wu, E.M., A general theory of strength for anisotropic materials. *J. Compos. Mater.*, 1971, **5**, 58–80.
75. Tsujimoto, Y. and Wilson, D., Elasto-plastic failure analysis of composite bolted joints. *J. Compos. Mater.*, 1986, **20**, 236–252.
76. Ye, L., Role of matrix resin in delamination onset and growth in composite laminates. *Compos. Sci. Technol.*, 1988, **33**, 257–277.
77. Hashin, Z. and Rotem, A., A fatigue failure criterion for fiber reinforced materials. *J. Compos. Mater.*, 1973, **7**, 448–464.
78. Robson, J., A survey of failure criteria, *Industrial Affiliates Review Paper*. Centre for Composite Materials, Imperial College, London, 1989.
79. Agarwal, B.L., Behaviour of multifastener bolted joints in composite materials.. *AIAA J.*, 1980, **80-0307**, 1–7.
80. Chang, F.K., Scott, R.A. and Springer, G.S., Failure of composite laminates containing pin loaded holes-method of solution. *J. Compos. Mater.*, 1984, **18**, 255–278.
81. Hyer, M.W. and Chastain, P.A., Effect of bolt load proportioning on the capacity of multiple-bolt composite joints. *J. Aircraft*, 1987, **25**, 184–189.
82. Ramakrishna, S., Hamada, H. and Nishiwaki, M., Bolted joints of pultruded sandwich composite laminates. *Compos. Structures*, 1995, **32**, 227–235.
83. Prabhakaran, R., Razzaq, Z. and Devara, S., Load and resistance factor design (LRFD) approach for bolted joints in pultruded composites. *Composites*, 1996, **27**, 351–360.
84. Hefferman, P.J. and Erki, M.A., Equivalent capacity and efficiency of reinforced-concrete beams strengthened with carbon-fiber-reinforced plastic sheets. *Can. J. Civil Engng.*, 1996, **23**, 21–29.
85. Mottram, J.T., Recommendations for the optimum design of pultruded frameworks. *Mech. Compos. Mater.*, 1996, **29**, 503–508.
86. Erki, M.A., Bolted glass-fiber-reinforced plastic joints. *Can. J. Civil Engng*, 1995, **2**, 736–744.
87. Bank, L.C., Mosallam, A.S. and McCoy, G.T., Design and performance of connections for pultruded frame structures. *J. Reinforced Plastics and Compos.*, 1994, **13**, 199–212.
88. Abdelnaby, S.F.M. and Hollaway, L., The experimental behaviour of bolted joints in pultruded glass polyester material: 1—single bolt joints. *Composites*, 1993, **24**, 531–538.
89. Abdelnaby, S.F.M. and Hollaway, L., The experimental behaviour of bolted joints in pultruded glass polyester material: 2—two bolt joints. *Composites*, 1993, **24**, 539–546.

90. Cooper, C. and Turvey, G.J., Effects of joint geometry and bolt torque on the structural performance of single bolt tension joints in pultruded GRP sheet material. *Compos. Structures*, 1995, **35**, 217–226.

APPENDIX A

NOMENCLATURE

w	laminate width
R	hole radius
e	end distance
d	hole diameter
t	laminate thickness
p	pitch
α	fibre orientation angle
θ	circumferential co-ordinate direction
φ	contact angle
c_d	diametral clearance
K_{tb}	tensile stress concentration factor
K_{sb}	shear stress concentration factor
S_b	bearing stress
μ	coefficient of friction
β	bearing to by-pass stress ratio
f_1	unevenness factor
P_b	load reacted at the hole
P_{bp}	by-pass load
S_{np}	by-pass stress
d_{0t}	tensile characteristic distance (point stress method)
d_{0c}	compressive characteristic distance (point stress method)
d_{0s}	shear characteristic distance (point stress method)
a_{0t}	tensile characteristic distance (average stress method)
a_{0c}	compressive characteristic distance (average stress method)
a_{0s}	shear characteristic distance (average stress method)
R_0	reference radius
S_c	ply shear strength
X_c	ply longitudinal compressive strength
X	ply longitudinal tensile strength
Y_c	ply transversal compressive strength
Y	ply transversal tensile strength
Z_{ij}	through the thickness shear strength
Z	through the thickness tensile strength
v	crack opening
G_c	total fracture energy developed in the damage zone
K_I	mode I stress intensity factor
K_{II}	mode II stress intensity factor
δ	fibre failure interaction zone
β_1	Weibull distribution shape parameter
E_{ii}	elastic moduli
G_{ij}	shear moduli
σ_{ij}	stresses
ν_{ij}	Poisson's ratios
D	washer diameter
T	torque
r_c	characteristic curve
α_1	shear strain–stress relation constant
γ_{xy}	shear strain
A	damage area